

Priming of CD8⁺ T Cells during Central Nervous System Infection with a Murine Coronavirus Is Strain Dependent[∇]

Katherine C. MacNamara,^{†‡} Susan J. Bender,[‡] Ming Ming Chua,
Richard Watson, and Susan R. Weiss*

Department of Microbiology, University of Pennsylvania School of Medicine, Philadelphia, Pennsylvania 19104

Received 15 January 2008/Accepted 6 April 2008

Virus-specific CD8⁺ T cells are critical for protection against neurotropic coronaviruses; however, central nervous system (CNS) infection with the recombinant JHM (RJHM) strain of mouse hepatitis virus (MHV) elicits a weak CD8⁺ T-cell response in the brain and causes lethal encephalomyelitis. An adoptive transfer model was used to elucidate the kinetics of CD8⁺ T-cell priming during CNS infection with RJHM as well as with two MHV strains that induce a robust CD8⁺ T-cell response (RA59 and SJHM/RA59, a recombinant A59 virus expressing the JHM spike). While RA59 and SJHM/RA59 infections resulted in CD8⁺ T-cell priming within the first 2 days postinfection, RJHM infection did not lead to proliferation of naïve CD8⁺ T cells. While all three viruses replicated efficiently in the brain, only RA59 and SJHM/RA59 replicated to appreciable levels in the cervical lymph nodes (CLN), the site of T-cell priming during acute CNS infection. RJHM was unable to suppress the CD8⁺ T-cell response elicited by RA59 in mice simultaneously infected with both strains, suggesting that RJHM does not cause generalized immunosuppression. RJHM was also unable to elicit a secondary CD8⁺ T-cell response in the brain following peripheral immunization against a viral epitope. Notably, the weak CD8⁺ T-cell response elicited by RJHM was unique to CNS infection, since peripheral inoculation induced a robust CD8⁺ T-cell response in the spleen. These findings suggest that the failure of RJHM to prime a robust CD8⁺ T-cell response during CNS infection is likely due to its failure to replicate in the CLN.

Members of the family *Coronaviridae* infect a wide range of mammalian species, including humans, and induce mild to severe disease of the respiratory tract, gastrointestinal tract, and central nervous system (CNS). Mouse hepatitis virus (MHV) infection provides a useful model for the study of acute and chronic CNS disease and specifically the process of demyelination, the hallmark of the human disease multiple sclerosis. Different strains of MHV induce disease with various degrees of severity. For example, CNS infection with the recombinant wild-type A59 (RA59) strain causes acute encephalitis during the first week of infection; a strong CD8⁺ T-cell response is observed in the brain, coinciding with viral clearance. However, despite clearance of infectious RA59 virus, demyelination develops, peaking at approximately 4 weeks postinfection (p.i.) (17, 20). In contrast, infection with the recombinant wild-type JHM (RJHM) strain (derived from the JHM isolate referred to as MHV-4 or JHM.SD [7, 28]) causes severe encephalomyelitis; the virus is not cleared, and mice typically succumb to disease by the end of the first week of infection. Furthermore, RJHM infection of the CNS elicits a very weak virus-specific CD8⁺ T-cell response in the brain (7, 20, 34). However, we have examined only the most virulent strain of JHM. It should be noted that there are other strains

of JHM that have deletions and mutations within the spike glycoprotein, rendering them less virulent and sometimes resulting in a change in cell tropism. The ability of neurotropic strains of MHV to replicate within cells of the CNS and cause disease of various degrees is ideal for allowing the dissection of both viral and host determinants of neuropathogenesis.

The spike glycoprotein of MHV is a major determinant of neurovirulence (32). It controls virus tropism and spread as it both binds the cellular receptor and induces fusion with target cells. In addition, it encodes neutralizing antibody epitopes and the H-2^b-restricted CD8⁺ T-cell epitopes recognized in C57BL/6 (B6) mice. The A59 spike differs from the JHM spike in that it contains a deletion of 52 amino acids within the hypervariable region. The hypervariable region has been well documented to tolerate mutation, but with attenuating effects on virulence (5, 7). RA59 and RJHM both encode an H-2K^b epitope at positions S598 to S605 (S598); however, due to the deletion, the A59 spike lacks the immunodominant H-2D^b epitope at positions S510 to S519 (S510). We previously selected isogenic recombinant viruses expressing the JHM spike in which all other genes are derived from the A59 strain of MHV (SJHM/RA59). The isogenic SJHM/RA59 virus has a 50% lethal dose (LD₅₀) similar to that of RJHM, demonstrating that the JHM spike is sufficient to generate a highly neurovirulent phenotype and an increased ability to spread within the CNS (32, 33). However, SJHM/RA59-infected mice exhibit slower kinetics of death than RJHM-infected mice, and notably, unlike RJHM, the chimeric SJHM/RA59 virus induces a strong CD8⁺ T-cell response in the brain (14, 34).

In addition to the spike, there is increasing evidence that other viral genes play important roles in pathogenesis. We (14,

* Corresponding author. Mailing address: Department of Microbiology, University of Pennsylvania School of Medicine, 36th Street and Hamilton Walk, Philadelphia, PA 19104-6076. Phone: (215) 898-8013. Fax: (215) 573-4858. E-mail: weissr@mail.med.upenn.edu.

[†] Present address: Wadsworth Center, 5094A David Axelrod Institute, 120 New Scotland Avenue, Albany, NY 12208.

[‡] K.C.M. and S.J.B. contributed equally to this work.

[∇] Published ahead of print on 16 April 2008.

21) and others (34, 35) have noted that the low CD8⁺ T-cell response observed during RJHM infection is not dependent on the spike, since the SJHM/RA59 recombinant induces a robust virus-specific CD8⁺ T-cell response. The difference between the CD8⁺ T-cell responses elicited by SJHM/RA59 and RJHM may explain why SJHM/RA59 kills mice more slowly than RJHM. Furthermore, the reverse chimeric recombinant virus expressing the A59 spike in the JHM background (SA59/RJHM) is unable to replicate in the liver despite the fact that it expresses the spike from the hepatotropic RA59 strain (27), suggesting that background genes play a significant role in viral tropism.

It is well established that virus-specific CD8⁺ T cells play a protective role against MHV and are essential for clearance of infectious virus from the CNS (6, 20, 40, 41). The effector mechanisms exerted by activated, virus-specific CD8⁺ T cells include the ability to secrete cytokines and the ability to lyse target cells. Gamma interferon (IFN- γ) expression is essential for clearance of MHV from the brain (3, 22, 29), and perforin-mediated lysis of infected cells also appears to play a role in viral clearance (6, 31). In contrast to infection with RA59 or the relatively neuroattenuated glial-cell-tropic strains of JHM, CNS infection with the highly neurovirulent RJHM strain results in very low levels of activated, virus-specific CD8⁺ T cells in the spleen and brain (14, 34). Furthermore, RJHM infection induces a different profile of cytokines and chemokines in the brains of infected mice than infection with RA59 (34, 35, 38). One dramatic difference is that RA59 infection results in a robust IFN- γ response whereas RJHM infection results in higher, sustained levels of IFN- β (34). These observations prompted us to address the following questions. (i) Does RJHM elicit a CD8⁺ T-cell response in the brain following intranasal (i.n.) inoculation, a route that requires more virus and results in slower infection than intracranial (i.c.) inoculation? (ii) What are the kinetics of CD8⁺ T-cell priming during CNS infections with RA59, SJHM/RA59, and RJHM? (iii) Is CNS infection with RJHM generally immunosuppressive? (iv) Do RA59, SJHM/RA59, and RJHM replicate efficiently in the draining cervical lymph nodes (CLN)? (v) Can RJHM elicit a secondary CD8⁺ T-cell response in the brain following peripheral immunization against a viral epitope? (vi) Is the low CD8⁺ T-cell response elicited during RJHM infection an inherent characteristic of the viral strain or specific to RJHM infection of the CNS? Our results suggest that RJHM fails to prime a CD8⁺ T-cell response specifically during infection of the CNS without causing generalized immunosuppression and that this lack of priming correlates with a low level of RJHM replication in the draining CLN, the site of CD8⁺ T-cell priming during acute CNS infection.

MATERIALS AND METHODS

Mice and viruses. Four- to 5-week-old male mice were used in all experiments. B6 and B6-LY5.2/Cr (CD45.1⁺) mice were obtained from the National Cancer Institute (Frederick, MD). P14 mice (CD45.2⁺) (4) were bred at the University of Pennsylvania. Recombinant MHV strains A59 (RA59) and JHM (RJHM), and a chimeric virus expressing the JHM spike in the A59 background (SJHM/RA59, originally referred to as S4R22), were selected by targeted recombination as described elsewhere (20, 32). Recombinant A59 and SJHM/RA59 expressing enhanced green fluorescent protein (EGFP) in place of nonessential gene 4 (referred to as RA59-gfp and SJHM/RA59-gfp, respectively) were selected by targeted recombination as previously described (37). RJHM-gfp was selected

using similar techniques. Selection of RA59-gfp expressing the H-2^b-restricted gp33 epitope of lymphocytic choriomeningitis virus (LCMV) fused to the N terminus of EGFP in place of gene 4 (referred to as RA59-gfp/gp33) is described in detail elsewhere (6). RJHM and SJHM/RA59 expressing the gp33 fusion were selected similarly via targeted recombination.

Inoculation of mice. For i.c. inoculations, mice were anesthetized with isoflurane, and the virus was injected into the left cerebral hemisphere in a total volume of 30 μ l phosphate-buffered saline (PBS) containing 0.75% bovine serum albumin (BSA). For i.n. inoculations, the virus was applied directly to the nostrils of a slightly anesthetized mouse in a total volume of 20 μ l PBS containing 0.75% BSA. For intraperitoneal (i.p.) inoculations, virus was injected in a total volume of 100 μ l PBS containing 0.75% BSA. Doses for individual experiments are indicated in the figure legends.

Isolation of mononuclear cells. Mononuclear cells were prepared from the brain as previously described (6, 30). Brains from four to six animals were pooled per group. Briefly, animals were perfused with 10 ml PBS. Brains were placed in ice-cold RPMI 1640 medium containing 10% fetal bovine serum (FBS) and were homogenized through a nylon mesh bag (pore diameter, 64 μ m) by using a syringe plunger. Cells were passed through a 30% Percoll gradient and then through a cell strainer (pore diameter, 70 μ m). The cell suspension was layered atop a 2-ml cushion of Lympholyte-M (Cedarlane Laboratories), and viable cells were removed from the interface, washed, and counted. Mononuclear cells were prepared from the spleen as previously described (6); this method was also used to isolate cells from the CLN. Briefly, tissues were homogenized through a nylon mesh bag (pore diameter, 64 μ m) in RPMI 1640 medium containing 1% FBS. Red blood cells were lysed with 0.83% NH₄Cl, and the remaining cells were washed and counted.

Intracellular cytokine staining and flow cytometry. Intracellular IFN- γ production was assayed in response to specific peptide stimulation as previously described (26, 33). Briefly, 1 \times 10⁶ brain- or spleen-derived mononuclear cells were cultured with 10 U of human recombinant interleukin-2 and 1 μ g/ml brefeldin A (Golgiplug; BD Biosciences) in the presence or absence of 1 μ g/ml peptide in a total volume of 200 μ l RPMI 1640 medium supplemented with 5% FBS for 5 h at 37°C. Cells were stained for surface expression of CD4, CD8, and/or CD45.2 using fluorescently conjugated monoclonal antibodies (BD Pharmingen). Cells were then fixed and permeabilized using the Cytofix/Cytoperm kit (BD Biosciences) and were stained with a fluorescein isothiocyanate-conjugated monoclonal rat anti-mouse IFN- γ antibody (BD Pharmingen). Cells were fixed in 2% paraformaldehyde and analyzed using a FACScan or FACSCalibur flow cytometer (Becton Dickinson). Total cell numbers per mouse were determined by multiplying the fraction of live cells positive for a given marker by the total number of live cells isolated per organ.

CFSE staining of spleen-derived mononuclear cells for adoptive transfer. Mononuclear cells were prepared from the spleens of P14 mice as described above. Cells were incubated with 5 μ M carboxyfluorescein succinimidyl ester (CFSE) for 10 min with periodic agitation. Staining was quenched by the addition of an equal volume of FBS, and cells were washed three times with PBS. Cells were then counted and resuspended in PBS for adoptive transfer into B6 mice. A total of 2 \times 10⁷ cells were injected intravenously (i.v.) into the lateral tail vein in a total volume of 0.5 ml PBS.

Mononuclear cell proliferation analysis. Mononuclear cells were isolated from the spleen or CLN as described above. Since CFSE labeling was performed on different days, it should be noted that the peak fluorescence intensity is not always the same; only those transfers performed on the same day can be compared. The proliferative index, the average number of divisions undergone by the divided population, was determined using FlowJo software (Tree Star, Inc.).

Virus replication in mice. To measure in vivo virus replication, mice were sacrificed and perfused with 10 ml PBS. Brains and/or CLN were placed in 1 to 3 ml of gel saline, an isotonic saline solution containing 0.167% gelatin; then they were weighed and stored frozen at -80°C. Tissues were subsequently homogenized, and standard plaque assays were performed on murine L2 fibroblast monolayers (13). Neutralization assays were performed using monoclonal antibodies raised against either the JHM spike (J7.2 and J7.18) or the A59 spike (A2.1); these antibodies were a kind gift from John Fleming (University of Wisconsin, Madison).

Listeria immunization. Recombinant *Listeria monocytogenes* strains expressing the H-2^b-restricted gp33-41 epitope (KAVYNFATC; referred to as gp33) or the H-2^d-restricted np118-126 epitope (RPQASGVYM; referred to as np118) from LCMV were engineered as previously described (36, 39). Both epitopes are expressed as fusion proteins with dihydrofolate reductase. Strain XFL703 expresses the gp33 epitope and is referred to below as rLm-gp33. Strain XFL303 expresses the np118 epitope and is referred to below as rLm-np118. Mice were

inoculated i.p. with 10^4 CFU of recombinant *L. monocytogenes* in 0.5 ml PBS, rested for 3 weeks, and then challenged i.c. with gp33-expressing strains of MHV.

RESULTS

RJHM elicits a weak virus-specific CD8⁺ T-cell response in the brain. i.c. inoculation of RJHM results in severe encephalitis, with high numbers of innate immune cells, including macrophages and neutrophils, being recruited into the brain parenchyma early during infection. However, the level of recruitment of T cells, both total and virus-specific CD8⁺ T cells, into the brain is extremely low (14, 34). One possibility that could account for the low CD8⁺ T-cell response in the brain following i.c. RJHM inoculation is that RJHM infection causes extensive tissue changes (more than those observed with SJHM/RA59) that prevent proper immune cell trafficking into or out of the brain. To address this issue, mice were inoculated with virus via the i.n. route, which results in slightly slower spread of virus within the brain and less tissue destruction during the first week of infection than i.c. inoculation. Mice inoculated i.n. do not succumb to the disease until after the first week of infection, thus allowing us to examine the antiviral T-cell response before massive tissue destruction occurs. It should be noted that the LD₅₀ for RJHM administered i.n. is approximately 2 log₁₀ units higher than that for RJHM administered i.c. In this experiment, all mice inoculated by the i.n. route survived the first 7 days of infection. However, like i.c. inoculation, i.n. infection with RJHM elicited a very weak CD8⁺ T-cell response in the brain (Fig. 1). This result was in contrast to infection with the chimeric SJHM/RA59 strain of MHV, which induced a robust CD8⁺ T-cell response to both H-2^b-restricted viral epitopes, S510 and S598 (Fig. 1). While the total number of cells isolated per brain from RJHM- and SJHM/RA59-infected mice differed only 2-fold (6.4×10^5 versus 1.3×10^6 , respectively), the number of CD8⁺ T cells isolated from RJHM-infected brains was nearly 50-fold lower than that for SJHM/RA59-infected brains (5.3×10^3 versus 2.6×10^5) (Fig. 1). The number of epitope-specific cells per brain was also significantly lower following RJHM infection than following SJHM/RA59 infection (Fig. 1). Thus, RJHM infection of the CNS elicits a weak CD8⁺ T-cell response in the brain following either i.c. or i.n. inoculation. Furthermore, this weak response is not solely dependent on the JHM spike. This difference in the CD8⁺ T-cell response between RJHM and SJHM/RA59 following i.n. inoculation is similar to what we have reported previously for i.c. inoculation (14), demonstrating that the minimal CD8⁺ T-cell response observed following i.c. inoculation of RJHM is not likely to be due to the rapid spread of virus and massive tissue destruction in the brain before a T-cell response can be elicited.

The kinetics of CD8⁺ T-cell priming during CNS infection with MHV is strain dependent. To assess the protective or pathogenic effects of virus-specific CD8⁺ T cells during the course of MHV disease, we previously developed an adoptive transfer system in which we could modulate the level of epitope-specific CD8⁺ T cells in vivo. This system utilized recombinant MHV strains expressing the gp33 epitope of LCMV and the transfer of gp33-specific CD8⁺ T cells from P14 transgenic mice. We previously observed that adoptive transfer of P14 splenocytes during the first 2 days after infec-

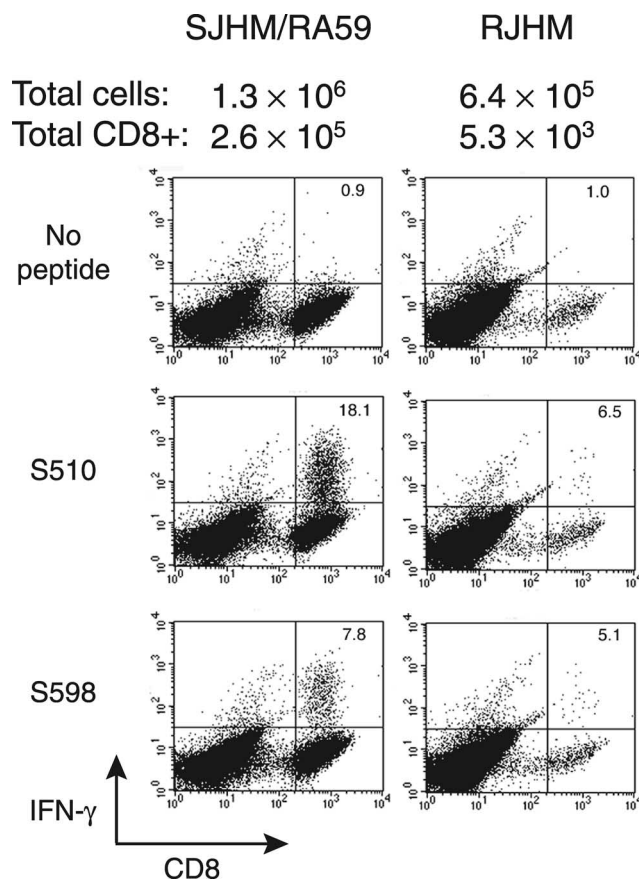


FIG. 1. Intranasal inoculation of RJHM elicits a weak CD8⁺ T-cell response in the brain. Brain lymphocytes harvested on day 7 p.i. from mice inoculated i.n. with 10^4 PFU of SJHM/RA59 or 10^3 PFU of RJHM were first stimulated with S510 and S598 peptides and then stained for intracellular IFN- γ in order to evaluate the virus-specific CD8⁺ T-cell response. The percentage of CD8⁺ T cells that are epitope specific, as determined by IFN- γ production, is given in the upper right quadrant of each plot. Data represent cells pooled from the brains of 4 to 6 animals per group and are representative of two independent experiments. The total numbers of live cells and CD8⁺ T cells harvested per brain are given above each column.

tion with RA59-gfp/gp33 can protect against disease; however, transfer on day 3 or 5 p.i. neither protects against nor enhances disease (20). Further analysis revealed that the P14 cells do not accumulate at the site of infection, the brain, when transferred at these later times; this result is in contrast to the dramatic accumulation of P14 cells within the brain when they are transferred early or prior to infection (20). We next aimed to determine the kinetics of CD8⁺ T-cell priming and, importantly, whether CD8⁺ T-cell priming was occurring during CNS infection with RJHM. Increasing the number of precursor cells by adoptive transfer allowed us to visualize CD8⁺ T-cell expansion and proliferation, and cell proliferation was used as an indicator of CD8⁺ T-cell priming. In this experiment, mice were inoculated with 10^4 PFU of RA59, SJHM/RA59, or RJHM expressing gfp/gp33. The gfp/gp33-expressing viruses are attenuated relative to their respective parental viruses, thus allowing inoculation of higher doses. On day 1, 2, or 3 p.i., P14 splenocytes were labeled with CFSE and transferred into the

infected mice. At 3 days posttransfer, cells were isolated from the spleen and CLN and were examined for CFSE dilution as an indicator of cell proliferation. Cells expressing low levels of CFSE (CFSE^{lo}) represent the divided population.

To analyze the proliferation of the transferred P14 cells (CD45.2⁺), we used CD45.1⁺ mice as transfer recipients, thus allowing us to identify CD8⁺ CD45.2⁺ cells as the transferred cells. The results of this experiment are shown in Fig. 2. As expected, the transferred cells did not proliferate and remained CFSE^{hi} in uninfected and RA59-gfp-infected animals (data not shown). During RA59-gfp/gp33 infection, when cells were transferred on day 1 p.i. and examined 3 days later, we observed that a significant number of the transferred CD8⁺ CD45.2⁺ cells underwent several rounds of division in both the CLN and the spleen, as indicated by dilution of CFSE (Fig. 2A). However, transfers performed on day 2 p.i. or later showed significantly lower percentages of proliferated cells, indicating that CD8⁺ T cells are primed within the first 2 days of RA59-gfp/gp33 infection. Importantly, the absence of proliferating cells in the animals receiving transfer on day 3 p.i. was not due to the presence of these cells in another location, since we have already shown that transferred cells are not present in the brains of these recipients (20). Similarly, infection with the chimeric gp33-expressing virus SJHM/RA59-gfp/gp33 resulted in early and robust CD8⁺ T-cell priming (Fig. 2B), consistent with the observation that this virus induces a strong CD8⁺ T-cell response (Fig. 1).

In sharp contrast, infection with RJHM-gfp/gp33 resulted in a dramatically different proliferation profile. Interestingly, little to no proliferation was observed in the populations of cells transferred on day 1, 2, or 3 p.i. (Fig. 2C). Thus, priming of naïve, virus-specific CD8⁺ T cells is greatly reduced during RJHM-gfp/gp33 infection relative to that with both RA59-gfp/gp33 and SJHM/RA59-gfp/gp33 infections. Importantly, this reduced response was not due to a lack of gp33 expression during infection with RJHM-gfp/gp33; sequencing of RNA from infected cells confirmed the presence of an intact gp33 sequence. Furthermore, EGFP, which is fused to the carboxyl terminus of the gp33 epitope, continued to be expressed in mice for at least 3 days p.i. (data not shown).

Reports indicate that CD8⁺ T cells are not infected by MHV *in vivo* (9); however, to confirm that donor CD8⁺ CD45.2⁺ cells were not infected with the EGFP-expressing recombinant viruses (and thus not contributing to the population of CFSE^{lo} cells), we harvested cells from the spleens and CLN of RA59-gfp/gp33- and RA59-gfp-infected animals that either did not receive adoptive transfer or received adoptive transfer of unlabeled P14 cells. As expected, these cells were negative for fluorescence in the FL1 channel (data not shown). Additionally, the experiments for which results are shown in Fig. 2 were repeated using an alternative dye, PKH26, which fluoresces in the FL2 channel, to confirm that the divided CFSE^{lo} population did not include MHV-infected CD8⁺ CD45.2⁺ cells (data not shown).

RJHM is not generally immunosuppressive. The induction of cytokines and chemokines in the brain has been shown to differ among different strains of MHV (34, 38). Based on these findings, we next investigated whether the RJHM-induced cytokine response could suppress the development of a virus-specific CD8⁺ T-cell response to RA59. To determine which

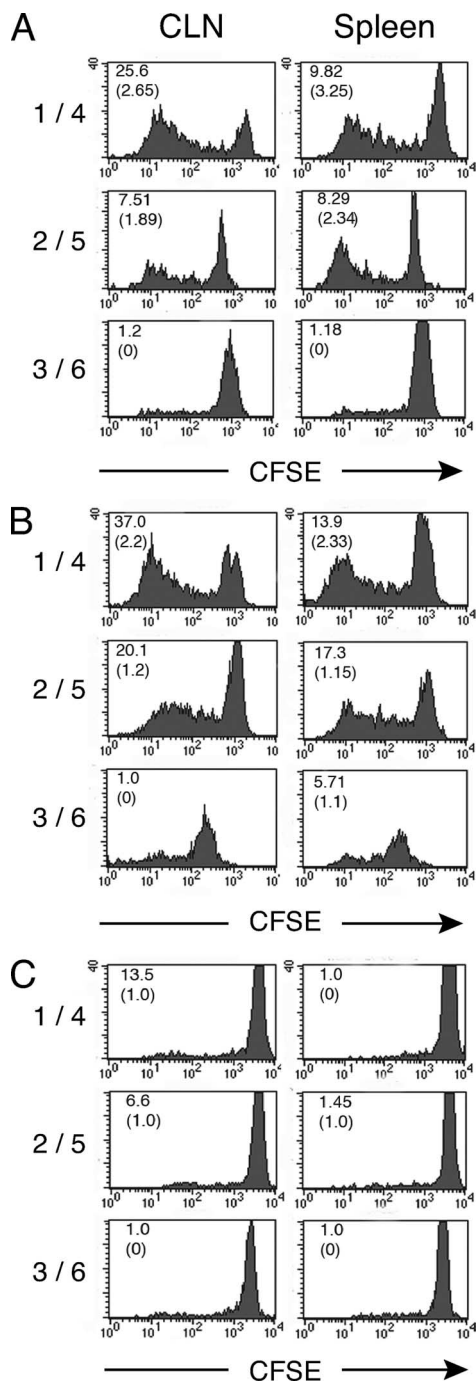


FIG. 2. Kinetics of naïve CD8⁺ T-cell priming. CD45.1⁺ mice inoculated i.c. with 10⁴ PFU of gfp/gp33-expressing virus received adoptive transfer of CFSE-labeled P14 cells on day 1, 2, or 3 p.i. Histograms represent transferred CD8⁺ CD45.2⁺ T cells. The percentage of transferred cells that have divided and (in parentheses) the proliferative index, which represents the average number of cell divisions that have occurred in the dividing population, are given at the upper left of each histogram. The proliferation of transferred cells in mice infected with RA59-gfp/gp33 (A), SJHM/RA59-gfp/gp33 (B), or RJHM-gfp/gp33 (C) is shown. The numbers to the left of each row indicate the days p.i. when cells were transferred/harvested. Each histogram represents data collected from a single mouse and is representative of the entire group (*n* = 3). Data are representative of two independent experiments.

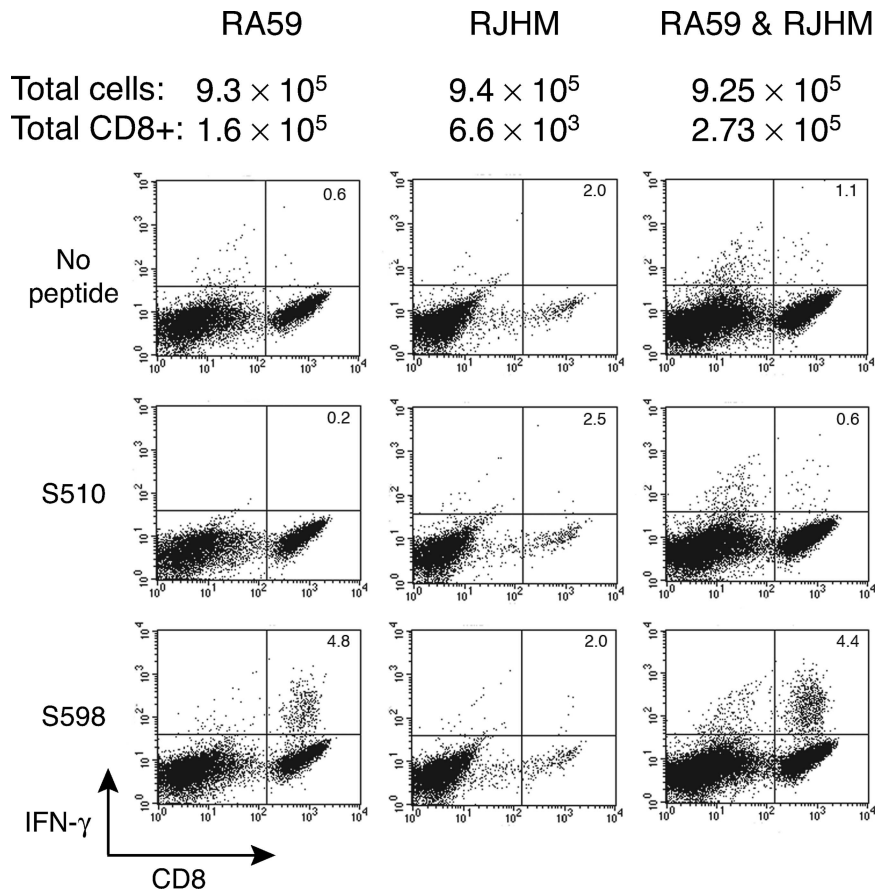


FIG. 3. RJHM inoculation does not suppress the CD8⁺ T-cell response elicited by RA59. Mice were inoculated i.c. with either 500 PFU of RA59, 10 PFU of RJHM, or both 500 PFU of RA59 and 10 PFU of RJHM; these doses represent approximately 1 LD₅₀ of RJHM and <1 LD₅₀ of RA59. Brain lymphocytes harvested on day 7 p.i. were stimulated with peptide and stained as for Fig. 1. The percentage of CD8⁺ T cells that are epitope specific, as determined by IFN- γ production, is given in the upper right quadrant of each plot. Data represent cells pooled from the brains of 4 to 6 animals per group and are representative of two independent experiments. The total numbers of live cells and CD8⁺ T cells harvested per brain are given above each column.

strain of MHV dominates the adaptive response, the weak CD8⁺ T-cell inducer RJHM or the robust CD8⁺ T-cell inducer RA59, we inoculated mice with both viral strains simultaneously and analyzed the CD8⁺ T-cell response in the brain at day 7 p.i. (Fig. 3).

The RA59 strain of MHV expresses only the subdominant S598 epitope, whereas RJHM expresses both S598 and the immunodominant S510 epitope. While similar numbers of mononuclear cells were isolated per brain from mice infected with either RA59 or RJHM (9.3×10^5 versus 9.4×10^5 , respectively), the total number of CD8⁺ T cells per brain was approximately 25-fold lower in the RJHM-infected animals (1.6×10^5 versus 6.6×10^3 , respectively) (Fig. 3). Furthermore, the S598-specific CD8⁺ T cells accounted for approximately 5% of the CD8⁺ T cells in RA59-infected mice, whereas RJHM infection resulted in minimal levels of S510- and S598-specific CD8⁺ T cells (Fig. 3). In contrast to infection with RJHM alone, coinfection with RA59 and RJHM resulted in significant recruitment of CD8⁺ T cells into the brain. While coinfecting mice exhibited a robust response (similar to RA59 infection in both percentages and total numbers) to S598, the epitope expressed by both RA59 and RJHM, there was no

appreciable response to the immunodominant S510 epitope, expressed only by RJHM (Fig. 3). Thus, under these conditions, the ability of RA59 to elicit a robust, virus-specific CD8⁺ T-cell response was dominant over the low CD8⁺ T-cell response induced by RJHM. Importantly, the striking observation that coinfection did not result in an S510-specific CD8⁺ T-cell response in the brain suggests that RJHM is unable to elicit a robust CD8⁺ T-cell response even in the presence of immune mediators governing an adaptive immune response to RA59.

In addition to analyzing the virus-specific CD8⁺ T-cell response in the brain, we also monitored survival in the coinfecting mice. As shown in Fig. 4A, the majority of mice coinfecting with RA59 and RJHM survived the infection, and those that died did so with slower kinetics than mice infected with RJHM alone, suggesting that some component of the host response elicited by RA59 is protective even in the context of infection with the destructive and highly lethal RJHM strain. To ensure that both viruses were indeed present within the brain and that preferential replication and spread of RA59 were not responsible for the RA59-like immune response, tissue homogenates were titrated for the presence of both RA59

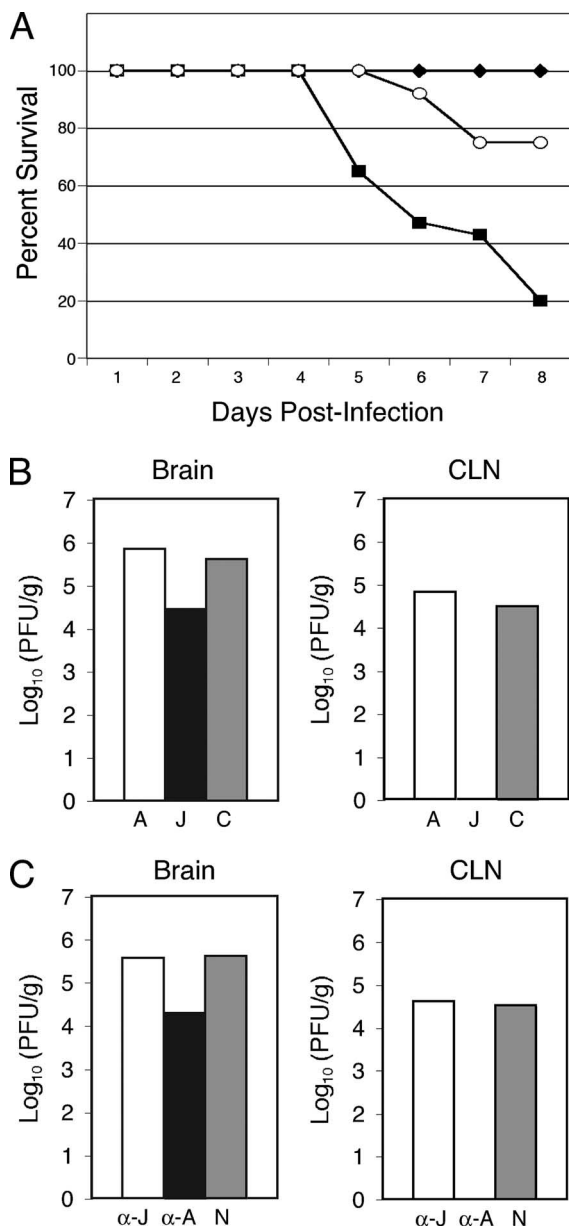


FIG. 4. Survival and virus replication in coinfecting mice. Mice were inoculated i.c. as described for Fig. 3. (A) The survival of infected mice was monitored for 10 mice per group. Mice coinfecting with RA59 and RJHM (open circles) displayed an intermediate survival phenotype relative to those of RJHM-infected (solid squares) and RA59-infected (solid diamonds) mice. (B) Virus replication in the brains and CLN of mice infected with RA59 (A) (open bars) or RJHM (J) (solid bar) or coinfecting with RA59 and RJHM (C) (shaded bars) was examined in tissues harvested on day 4 p.i. Tissue homogenates were titrated on L2 fibroblasts. Bars represent mean viral titers (3 mice per group). (C) Brain and CLN homogenates from coinfecting animals were used in a neutralization assay using a monoclonal antibody specific for either the A59 spike (A2.1) or the JHM spike (J7.2 and J7.18). Tissue homogenates were incubated with a 1:10 dilution of anti-JHM antibody (α -J) (open bars), anti-A59 antibody (α -A) (solid bars), or no antibody (N) (shaded bars) for 1 h prior to the performance of standard plaque assays. (The CLN from all RJHM-infected mice had titers below the limit of detection.)

and RJHM (Fig. 4B). At day 4 p.i., which is close to the peak of virus replication in vivo, brains and CLN were harvested from coinfecting mice. The CLN were evaluated to determine if both RA59- and RJHM-infected cells were present at the site where CD8⁺ T-cell priming is thought to occur during acute MHV infection of the CNS.

At day 4 p.i., viral titers in the brains of RA59-infected mice were significantly higher than those in RJHM-infected brains (Fig. 4B). Interestingly, RA59 also replicated to relatively high titers in the CLN, whereas RJHM titers were below the limit of detection (Fig. 4B). The titers observed in coinfecting mice appeared to mirror those observed in mice infected with RA59 or RJHM alone (Fig. 4B). However, to confirm that both RA59 and RJHM were indeed replicating in the brains of coinfecting animals, a neutralization assay was performed in which brain homogenates from coinfecting animals were incubated with monoclonal antibodies specific for either the A59 spike (A2.1) or the JHM spike (J7.2 and J7.18) prior to the performance of standard plaque assays. This allowed selective detection of either RA59 or RJHM. While both RA59 and RJHM were present in the brains of coinfecting animals, only RA59 replicated to measurable titers within the CLN (Fig. 4C). This difference in RA59 and RJHM replication in the draining CLN correlates with the difference in CD8⁺ T-cell priming observed during these infections.

RJHM replicates poorly in the CLN compared to RA59 and SJHM/RA59. The difference in viral titers in the CLN of RA59- and RJHM-infected mice at day 4 p.i. (Fig. 4C) suggested that the poor CD8⁺ T-cell priming during RJHM infection could be due, at least in part, to the absence of infectious virus in the CLN, the site of priming during acute MHV infection of the CNS. Thus, we further compared the replication of RA59, SJHM/RA59, and RJHM in the draining CLN to determine whether RJHM replicates in the CLN at early times postinfection, when priming is thought to occur. Mice were infected with 50 PFU of RA59, SJHM/RA59, or RJHM, and infectious virus was titrated from the brain and CLN on days 1 to 5 p.i. While all three viruses replicated efficiently in the brain during the course of 5 days p.i. (Fig. 5A), only RA59 and SJHM/RA59 replicated to appreciable titers in the CLN during this time, while RJHM replicated only to a minimal extent (Fig. 5B). Thus, the ability of these strains to prime an effective CD8⁺ T-cell response correlates with the presence of infectious virus in the draining CLN. Interestingly, the replication of RJHM in the brain was lower than those of RA59 and SJHM/RA59 during the first 2 days p.i. (Fig. 5A), the time during which priming occurs (Fig. 2). These data suggest that the minimal CD8⁺ T-cell priming observed during RJHM infection of the CNS may be due to a lack of RJHM antigen in the CLN, the site of T-cell priming during acute CNS infection.

RJHM elicits a weak secondary CD8⁺ T-cell response in the brain after immunization against a viral epitope. To further investigate the mechanism by which RJHM fails to elicit a robust CD8⁺ T-cell response in the brain, we next asked whether RJHM infection could elicit a strong secondary response in the brain following peripheral immunization against a single viral epitope. Since the S510- and S598-specific CD8⁺ T-cell responses differ for RA59 and RJHM, we instead utilized the gp33 epitope and the gfp/gp33-expressing MHV strains for this experiment. Immunization was performed using

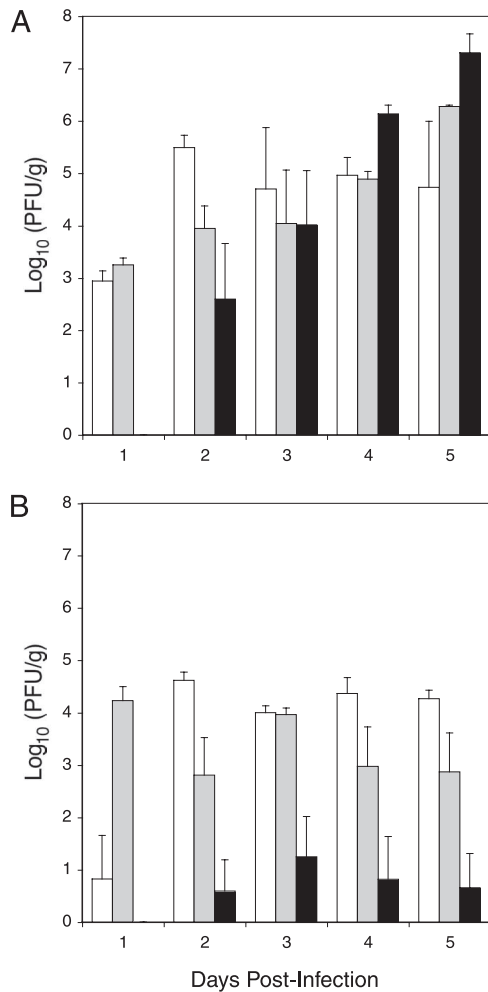


FIG. 5. RJHM replicates inefficiently in the draining CLN. Mice were inoculated with 50 PFU of RA59 (open bars), SJHM/RA59 (shaded bars), or RJHM (solid bars). Brains (A) and CLN (B) were removed on days 1 to 5 p.i., and tissue homogenates were titrated on L2 fibroblasts to assess viral replication. Bars represent mean viral titers (5 mice per group). Error bars, standard errors of the means. (Individual tissues with no measurable titer were assigned a log₁₀ value of zero.) Data shown are representative of two independent experiments.

two recombinant *Listeria monocytogenes* strains engineered to express either the gp33 epitope (expressed by recombinant gfp/gp33-expressing MHV strains) or the nonspecific np118 epitope (not expressed by these MHV strains) of LCMV. Mice were inoculated i.p. with 10⁴ CFU of rLm-gp33 or rLm-np118, rested for 3 weeks, and then challenged i.c. with approximately 1 LD₅₀ of either RA59-gfp/gp33 or RJHM-gfp/gp33. Since a secondary immune response typically occurs more rapidly than a primary response, mice were sacrificed at day 5 p.i., and brain lymphocytes were analyzed to assess the magnitude of the CD8⁺ T-cell response. While the total number of live cells per brain differed less than twofold among all groups, striking differences were observed in the number of CD8⁺ T cells per brain (Fig. 6A and B). While RA59-gfp/gp33-infected mice immunized with nonspecific *Listeria* yielded approximately 9.66 × 10⁴ CD8⁺ T cells per brain at 5 days p.i. (representing

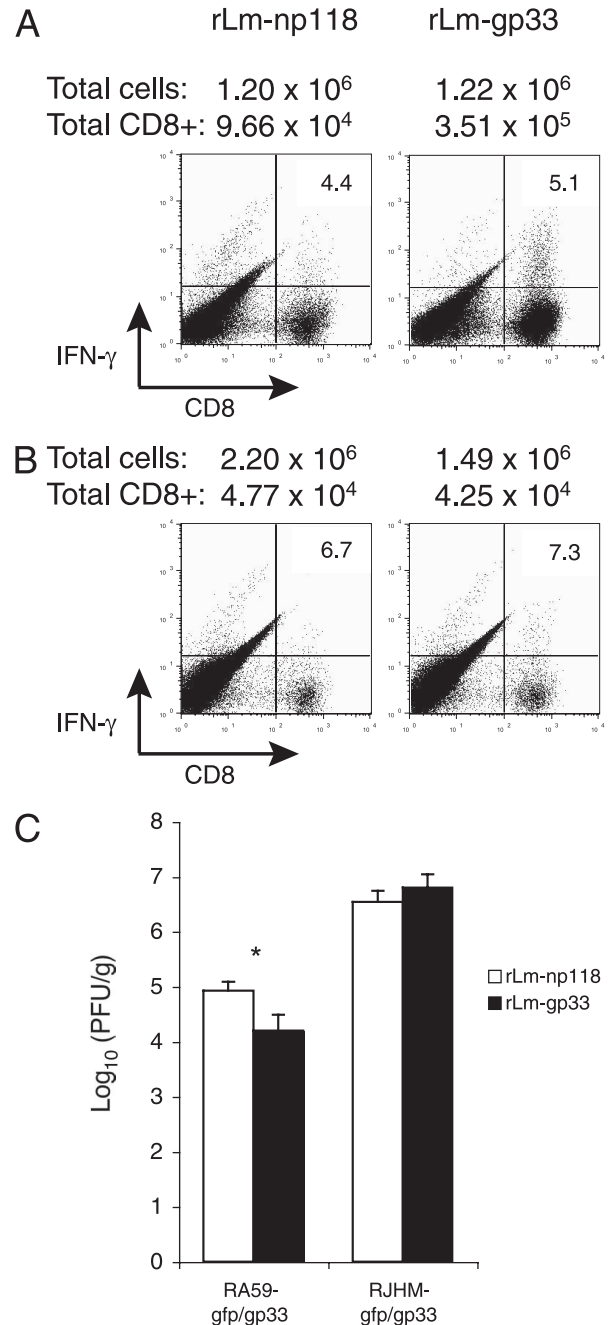


FIG. 6. RJHM fails to elicit a robust secondary response in the brain following peripheral immunization against a viral epitope. Mice were inoculated i.p. with 10⁴ CFU of rLm-np118 or rLm-gp33, rested for 3 weeks, and then challenged i.c. with 10⁵ PFU of RA59-gfp/gp33 (A) or 10³ PFU of RJHM-gfp/gp33 (B). Brain lymphocytes were harvested on day 5 p.i., stimulated with gp33 peptide, and stained as for Fig. 1. The percentage of CD8⁺ T cells that are epitope specific, as determined by IFN-γ production, is given in the upper right quadrant of each plot. Data represent cells pooled from the brains of 4 to 6 animals per group and are representative of three similar experiments. The total numbers of live cells and CD8⁺ T cells harvested per brain are given above each column. (C) Virus replication in the brain was examined on day 5 p.i. Tissue homogenates were titrated on L2 fibroblasts. Bars represent mean viral titers (3 mice per group). Error bars, standard errors of the means (*, *P* = 0.04).

approximately 8.09% of the live cells recovered), mice immunized with rLm-gp33 showed a significantly greater response (3.51×10^5 CD8⁺ T cells per brain, representing approximately 29.61% of live cells) (Fig. 6A). In sharp contrast, mice infected with RJHM-gfp/gp33 showed little to no difference in the CD8⁺ T-cell response following immunization with rLm-gp33 compared to nonspecific *Listeria* (approximately 2.87% versus 2.25% CD8⁺ T cells, respectively) (Fig. 6B). Importantly, the secondary CD8⁺ T-cell response elicited by RJHM-gfp/gp33 following rLm-gp33 immunization was significantly lower than the secondary response elicited by RA59-gfp/gp33, both in total numbers and in percentages (2.87% versus 29.61% CD8⁺ T cells, respectively) (Fig. 6A and B). Since the percentages of CD8⁺ T cells specific for gp33 were similar in all cases, the absolute number of gp33-specific CD8⁺ T cells elicited during the secondary response to RJHM-gfp/gp33 was no greater than the response in mice immunized with nonspecific *Listeria* and was significantly lower than the secondary response to RA59-gfp/gp33 (Fig. 6A and B). Thus, while RA59-gfp/gp33 induced a robust secondary response in the brain following peripheral immunization against a viral epitope, RJHM-gfp/gp33 was deficient in this ability.

To verify that the lack of a CD8⁺ T-cell response in RJHM-gfp/gp33-infected mice following peripheral immunization was not due to poor replication of RJHM-gfp/gp33 in the brain, tissue homogenates from infected mice were titrated at day 5 p.i. As shown in Fig. 6C, RJHM-gfp/gp33 replicated to higher titers than RA59-gfp/gp33 in the brains of infected mice, demonstrating that the poor secondary CD8⁺ T-cell response to RJHM-gfp/gp33 is not due to poor viral replication in the brain. Furthermore, immunization with rLm-gp33 did not reduce the amount of replication in the brains of RJHM-gfp/gp33-infected mice relative to that for rLm-np118-immunized mice (Fig. 6C); this is not surprising, given the very small numbers of gp33-specific CD8⁺ T cells infiltrating the brain (Fig. 6B). There was, however, an approximately 10-fold reduction in RA59-gfp/gp33 titers ($P = 0.04$) when mice were immunized with rLm-gp33 compared to rLm-np118, a finding similar to what we have observed previously (6).

RJHM elicits a robust CD8⁺ T-cell response in the spleen following peripheral inoculation. Since CNS infection with RJHM elicits a weak virus-specific CD8⁺ T-cell response in the brain, we next aimed to determine if this feature was inherent to the virus or a unique characteristic of CNS infection. To address this issue, mice were inoculated with RA59, SJHM/RA59, or RJHM via the i.p. route. Spleen lymphocytes were analyzed on day 8 p.i. (the peak of the CD8⁺ T-cell response following inoculation by this route) to assess the magnitude of the response. As expected, i.p. inoculation with RA59 elicited a robust CD8⁺ T-cell response to S598 in the spleen (Fig. 7A). Interestingly, both SJHM/RA59 and RJHM elicited robust responses to epitopes S510 and S598 following i.p. inoculation (Fig. 7A). Total numbers of viable splenocytes per mouse as well as CD8⁺ T cells per spleen were not statistically different for any of the viruses examined (Fig. 7B). Similarly, no statistical difference was observed in total numbers of S510-specific (SJHM/RA59 and RJHM only) and S598-specific CD8⁺ T cells harvested per spleen (Fig. 7B). Thus, the RJHM strain of MHV induces a robust virus-specific CD8⁺

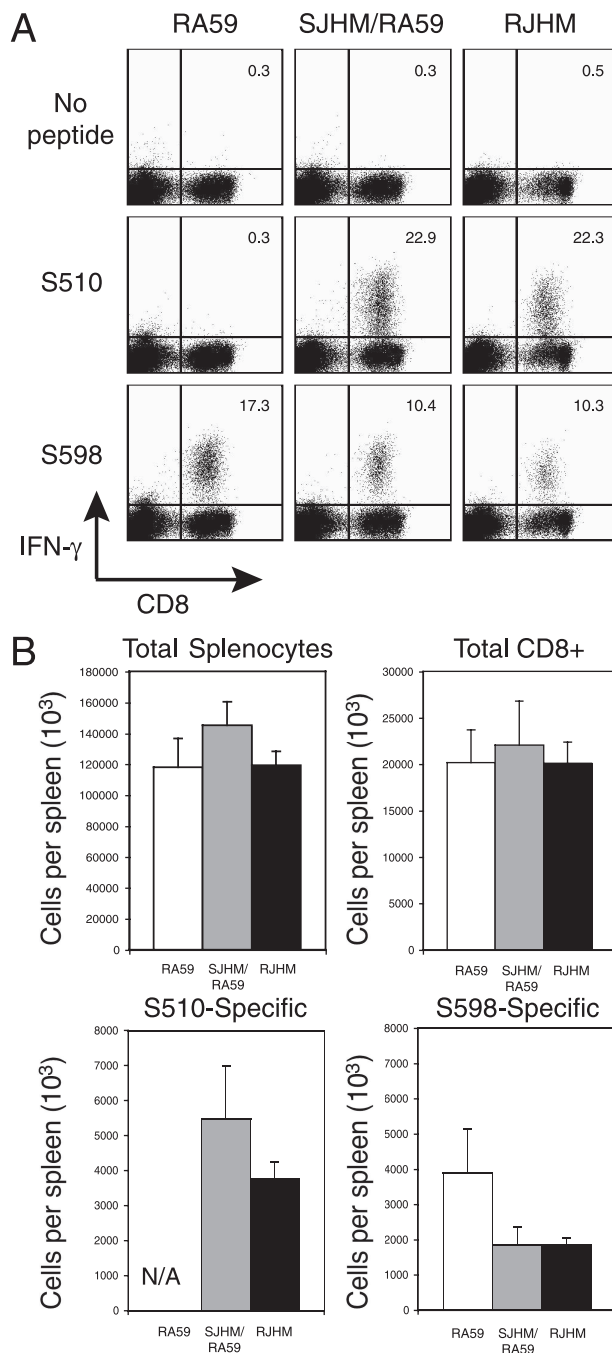


FIG. 7. Intrapertitoneal inoculation of RJHM elicits a robust CD8⁺ T-cell response in the spleen. (A) Spleen lymphocytes harvested on day 8 p.i. from mice inoculated i.p. with 10^4 PFU of RA59, SJHM/RA59, or RJHM were stimulated with peptide and stained as for Fig. 1. The percentage of CD8⁺ T cells that are epitope specific, as determined by IFN- γ production, is given in the upper right quadrant of each plot. Each column represents cells harvested from one individual mouse and is representative of the entire group ($n = 4$). (B) Total numbers of live cells, CD8⁺ T cells, and S510- and S598-specific CD8⁺ T cells per spleen were compared for each virus. Bars indicate the mean value for each group ($n = 4$). Error bars, standard errors of the means. All P values were >0.10 , as determined by one-way analysis of variance. Data shown are representative of two independent experiments.

T-cell response when inoculated i.p. This result is in sharp contrast to the response observed following CNS infection.

DISCUSSION

The presence of CD8⁺ T cells in the CNS during infection with neurotropic strains of MHV has been implicated in both protection and pathogenesis. While virus-specific CD8⁺ T cells likely contribute to the pathogenesis of demyelination through the secretion of macrophage-recruiting cytokines (34), their role in protection and clearance of infectious virus appears to outweigh their detrimental effects. This protective role is illustrated by the remarkable susceptibility of β_2 -microglobulin-deficient mice to infection with RA59 (10). Furthermore, we speculate that the lethality of the highly neurovirulent RJHM strain of MHV may be due, at least in part, to the poor CD8⁺ T-cell response elicited by this virus after i.c. (14) or i.n. (Fig. 1) inoculation. A similarly low CD8⁺ T-cell response has also been reported in response to JHM.SD (MHV-4), a closely related JHM isolate (34). The data presented here suggest that during CNS infection RJHM is largely able to avoid CD8⁺ T-cell priming and that this ability leads to the poor CD8⁺ T-cell response observed in the brains of RJHM-infected mice. Importantly, this finding appears to be unique to CNS infection with RJHM, since i.p. inoculation resulted in a robust virus-specific CD8⁺ T-cell response in the spleen (Fig. 7). Furthermore, the poor CD8⁺ T-cell response during CNS infection with RJHM does not appear to be a function of disease severity, as illustrated by i.n. infection (Fig. 1) and coinfection (Fig. 3), both of which were less severe than i.c. infection with RJHM alone. In addition, a chimeric recombinant expressing the A59 spike within the background of RJHM causes a very mild infection and still fails to induce a CD8⁺ T-cell response (14). The poor CD8⁺ T-cell response during CNS infection with RJHM also appears to be independent of the viral dose, since very high doses of RJHM-gfp/gp33 were used in the priming experiments (Fig. 2) and doses as low as 20 PFU of RA59 given i.c. induce a robust CD8⁺ T-cell response in the brain (14).

Since minimal priming of virus-specific CD8⁺ T cells was observed in RJHM-infected mice (Fig. 2), we further investigated whether activated CD8⁺ T cells transferred into RJHM-gfp/gp33-infected mice could traffic to the infected CNS and protect against neurological disease. To this end, P14 splenocytes were transferred into B6 mice and activated *in vivo* with rLm-gp33. Activated P14 cells were then transferred to naïve B6 mice, and these recipients were infected with RA59-gfp/gp33 or RJHM-gfp/gp33. Analysis of brain lymphocytes on day 7 p.i. demonstrated that activated P14 cells trafficked efficiently to the brains of RA59-gfp/gp33-infected mice, while only small numbers of activated cells were present in the brains of RJHM-gfp/gp33-infected mice (data not shown). Furthermore, those RJHM-gfp/gp33-infected mice that received adoptive transfer of activated cells showed clinical signs and mortality similar to those of controls that did not receive transfer (data not shown). While transfer of activated virus-specific CD8⁺ T cells was unable to protect mice from RJHM-induced neurological disease, such experiments are complicated by the low levels of T-cell-recruiting cytokines expressed in the brain following RJHM infection compared to RA59 infection (34, 38).

Thus, RJHM may avoid the induction of a CD8⁺ T-cell response in the brain due to both an inefficiency of priming and an inability to recruit activated cells to the CNS.

Many studies have demonstrated that a robust adaptive immune response can be mounted to antigens expressed in the brain. While antigen presentation during some chronic infections can occur within the brain itself (24), the ability to recruit an adaptive immune response during acute CNS infection relies on antigen presentation in the draining CLN (15, 23, 25). Soluble antigen injected directly into the brains of mice reaches the CLN within minutes to hours (11, 19). The development and migration of a protective CD8⁺ T-cell response has been examined for several CNS infections and likely depends on the pathogenic organism. Mice infected with an attenuated variant of JHM (J2.2 v-1) that primarily infects glial cells were used to characterize the trafficking of CD8⁺ T cells into the CNS during acute infection (23). Interestingly, in contrast to the highly neurovirulent RJHM strain used in our studies, J2.2 v-1 induces a robust antiviral CD8⁺ T-cell response. As with RA59, CNS infection with J2.2 v-1 results in a high percentage of virus-specific CD8⁺ T cells in the brain during the acute stage of disease. Using tetramers specific for the immunodominant S510 epitope, it was determined that the initial expansion of CD8⁺ T cells occurs in the CLN, followed by further expansion of virus-specific CD8⁺ T cells in the spleen and eventual accumulation in the brain (23). In this model, only highly activated CD8⁺ T cells are evident in the brain. The data from our T-cell-priming experiments are in agreement with this finding, since only CFSE-negative P14 cells were detected in the brains of infected mice (data not shown).

In a mouse model using ocular infection with herpes simplex virus type 1 and the adoptive transfer of epitope-specific CD8⁺ T cells, the site of T-cell priming was determined to be the submandibular lymph node (16). Interestingly, however, when cells are transferred 1 day prior to infection with herpes simplex virus type 1, proliferation cannot be detected until day 5 p.i.; these kinetics are delayed compared to what we observed during infection with RA59-gfp/gp33 (Fig. 2A) and raise the question of what factors contribute to the kinetics of T-cell priming. Important factors likely include the tropism of the infectious organism, the kinetics of infection, the route of inoculation, and the potential interactions of the infectious organism with antigen-presenting cells (APC). Each of these factors may influence antigen distribution and availability, the rate at which APC encounter antigens, and thus the length of time it takes them to interact with naïve CD8⁺ T cells, and/or the capacity of APC to present antigens and provide appropriate costimulation. The poor CD8⁺ T-cell priming observed during acute infection with RJHM-gfp/gp33 compared to infection with RA59-gfp/gp33 (Fig. 2), the lack of response to S510 in mice coinfecting with RA59 and RJHM (Fig. 3), and the inability of RJHM to elicit a robust secondary response in the brain (Fig. 6) together suggest an inefficiency of RJHM antigen presentation that may be due to viral effects on the APC and/or an inaccessibility of RJHM antigen.

The data presented here support the hypothesis that the poor CD8⁺ T-cell priming observed during RJHM infection of the CNS likely results from an inaccessibility of RJHM antigen to APC in the CLN rather than from a direct effect on APC

function. The data in Fig. 2 and 5 show that the ability to prime a CD8⁺ T-cell response correlates with viral replication in the CLN during the first 2 days p.i., when antigen presentation is taking place. RJHM replicates very poorly in the CLN compared with RA59 and SJHM/RA59, while all three viruses replicate to high titers in the brain. Furthermore, RJHM induces a robust CD8⁺ T-cell response when inoculated i.p. (Fig. 7). While little is known about the site of replication or the site of T-cell priming following i.p. inoculation with MHV, dendritic cells (DC) are believed to be the relevant APC following inoculation by this route (43), thus arguing against an interaction of RJHM with DC that prevents priming. Furthermore, we compared the phenotype of DC present in the CLN of mice infected with RA59 and RJHM on days 1 to 3 p.i. and were unable to detect any differences in DC activation despite an increase in CD11c⁺ cells in the CLN of both RA59- and RJHM-infected mice (data not shown); this increase in DC numbers was similar to that reported for CNS infection with an attenuated variant of JHM (J2.2 v-1) (42). Nevertheless, we cannot exclude the possibility that there may be other phenotypic or functional differences between DC from RA59- and RJHM-infected mice that could contribute to the differences in T-cell priming. Finally, the observation that coinfecting mice mount a robust CD8⁺ T-cell response to RA59 even in the presence of RJHM infection (Fig. 3) indicates that RJHM is not generally immunosuppressive; thus, RJHM does not appear to alter the cytokine milieu in the brain or CLN in a way that compromises antigen presentation.

We further speculate that a lack of antigen availability to APC in the CLN may be linked to the cellular tropism of RJHM. The highly neurovirulent RJHM strain of MHV is thought to predominantly infect neurons (8), in contrast to the less neurovirulent JHM strains and RA59, which are more glial-cell tropic and induce a robust CD8⁺ T-cell response. Indeed, we have observed that RJHM spreads more extensively than RA59 in primary neuronal cells in vitro (data not shown). Infected neurons are less likely to lyse and release viral antigen than other CNS cell types, due to their ability to prevent apoptosis (reviewed in reference 2), and cell-mediated lysis of infected neurons is limited by their low surface expression of major histocompatibility complex class I molecules. Thus, mechanisms that preserve neuronal integrity in the face of viral infection may limit the availability of RJHM antigen to be taken up and presented by APC via cross-presentation pathways. Furthermore, MHV may drain directly from the CNS, via lymphatics, to the CLN (1), where it is then able to infect APC. It was recently shown that, following peripheral infection, both vaccinia virus and vesicular stomatitis virus rapidly reach the draining lymph nodes via lymphatics and infect DC, which then present antigens to T cells (12). While infectious RJHM is present in the brains of infected mice (Fig. 5 and 6), titers are comparatively low at early times p.i., when T-cell priming takes place (Fig. 5). If RJHM is indeed highly neuronal, it may be highly cell associated, since primary neurons infected in vitro produce less infectious virus than other CNS cell types (18, 33). In contrast, RA59 infection of diverse CNS cell types, such as microglia/macrophages and astrocytes, as well as the measurable replication of RA59 in the draining CLN (Fig. 4 and 5), likely yields higher levels of viral antigen for presentation by APC. Studies are currently under way to

determine if RJHM infection of the CNS is indeed primarily restricted to neurons (8), particularly at early times p.i., before T-cell priming occurs.

The data presented here demonstrate that closely related neurotropic strains of MHV have a differential ability to induce a CD8⁺ T-cell response during CNS infection. We suggest that the decreased ability of RJHM to induce a CD8⁺ T-cell response in the brain leads to a lack of viral clearance and thus contributes to the high neurovirulence of RJHM compared to RA59. Notably, this feature appears to be unique to RJHM infection of the CNS, since i.p. inoculation of RJHM induces a robust CD8⁺ T-cell response in the periphery. The precise mechanism by which RJHM avoids the induction of a protective antiviral CD8⁺ T-cell response during CNS infection is an area of ongoing research.

ACKNOWLEDGMENTS

This work was supported by NIH grants AI-60021 and AI-47800 to S.R.W. K.C.M. was partially supported by NIH training grant AI-07324 and S.J.B. by NIH training grants GM-07170 and NS-07180.

REFERENCES

1. Barthold, S. W., and A. L. Smith. 1992. Viremic dissemination of mouse hepatitis virus-JHM following intranasal inoculation of mice. *Arch. Virol.* **122**:35–44.
2. Benn, S. C., and C. J. Woolf. 2004. Adult neuron survival strategies—slamming on the brakes. *Nat. Rev. Neurosci.* **5**:686–700.
3. Bergmann, C. C., B. Parra, D. R. Hinton, R. Chandran, M. Morrison, and S. A. Stohman. 2003. Perforin-mediated effector function within the central nervous system requires IFN- γ -mediated MHC up-regulation. *J. Immunol.* **170**:3204–3213.
4. Brändle, D., K. Burki, V. A. Wallace, U. H. Rohrer, T. W. Mak, B. Malissen, H. Hengartner, and H. Pircher. 1991. Involvement of both T cell receptor V α and V β variable region domains and α chain junctional region in viral antigen recognition. *Eur. J. Immunol.* **21**:2195–2202.
5. Buchmeier, M. J., H. A. Lewicki, P. J. Talbot, and R. L. Knobler. 1984. Murine hepatitis virus-4 (strain JHM)-induced neurologic disease is modulated in vivo by monoclonal antibody. *Virology* **132**:261–270.
6. Chua, M. M., K. C. MacNamara, L. San Mateo, H. Shen, and S. R. Weiss. 2004. Effects of an epitope-specific CD8⁺ T-cell response on murine coronavirus central nervous system disease: protection from virus replication and antigen spread and selection of epitope escape mutants. *J. Virol.* **78**:1150–1159.
7. Dalziel, R. G., P. W. Lampert, P. J. Talbot, and M. J. Buchmeier. 1986. Site-specific alteration of murine hepatitis virus type 4 peplomer glycoprotein E2 results in reduced neurovirulence. *J. Virol.* **59**:463–471.
8. Fazakerley, J. K., S. E. Parker, F. Bloom, and M. J. Buchmeier. 1992. The V5A13.1 envelope glycoprotein deletion mutant of mouse hepatitis virus type-4 is neuroattenuated by its reduced rate of spread in the central nervous system. *Virology* **187**:178–188.
9. Godfraind, C., K. V. Holmes, and J. P. Coutelier. 1995. Thymus involution induced by mouse hepatitis virus A59 in BALB/c mice. *J. Virol.* **69**:6541–6547.
10. Gombold, J. L., R. M. Sutherland, E. Lavi, Y. Paterson, and S. R. Weiss. 1995. Mouse hepatitis virus A59-induced demyelination can occur in the absence of CD8⁺ T cells. *Microb. Pathog.* **18**:211–221.
11. Gordon, L. B., P. M. Knopf, and H. F. Cserr. 1992. Ovalbumin is more immunogenic when introduced into brain or cerebrospinal fluid than into extracerebral sites. *J. Neuroimmunol.* **40**:81–87.
12. Hickman, H. D., K. Takeda, C. N. Skon, F. R. Murray, S. E. Hensley, J. Loomis, G. N. Barber, J. R. Bennink, and J. W. Yewdell. 2008. Direct priming of antiviral CD8⁺ T cells in the peripheral interfollicular region of lymph nodes. *Nat. Immunol.* **9**:155–165.
13. Hingley, S. T., J. L. Gombold, E. Lavi, and S. R. Weiss. 1994. MHV-A59 fusion mutants are attenuated and display altered hepatotropism. *Virology* **200**:1–10.
14. Iacono, K. T., L. Kazi, and S. R. Weiss. 2006. Both spike and background genes contribute to murine coronavirus neurovirulence. *J. Virol.* **80**:6834–6843.
15. Karman, J., C. Ling, M. Sandor, and Z. Fabry. 2004. Initiation of immune responses in brain is promoted by local dendritic cells. *J. Immunol.* **173**:2353–2361.
16. Lang, A., and J. Nikolich-Zugich. 2005. Development and migration of protective CD8⁺ T cells into the nervous system following ocular herpes simplex virus-1 infection. *J. Immunol.* **174**:2919–2925.

17. Lavi, E., D. H. Gilden, Z. Wroblewska, L. B. Rorke, and S. R. Weiss. 1984. Experimental demyelination produced by the A59 strain of mouse hepatitis virus. *Neurology* **34**:597–603.
18. Lavi, E., A. Suzumura, M. Hirayama, M. K. Highkin, D. M. Dambach, D. H. Silberberg, and S. R. Weiss. 1987. Coronavirus mouse hepatitis virus (MHV)-A59 causes a persistent, productive infection in primary glial cell cultures. *Microb. Pathog.* **3**:79–86.
19. Ling, C., M. Sandor, and Z. Fabry. 2003. In situ processing and distribution of intracerebrally injected ova in the CNS. *J. Neuroimmunol.* **141**:90–98.
20. MacNamara, K. C., M. M. Chua, P. T. Nelson, H. Shen, and S. R. Weiss. 2005. Increased epitope-specific CD8⁺ T cells prevent murine coronavirus spread to the spinal cord and subsequent demyelination. *J. Virol.* **79**:3370–3381.
21. MacNamara, K. C., M. M. Chua, J. J. Phillips, and S. R. Weiss. 2005. Contributions of the viral genetic background and a single amino acid substitution in an immunodominant CD8⁺ T-cell epitope to murine coronavirus neurovirulence. *J. Virol.* **79**:9108–9118.
22. Marten, N. W., M. Hohman, S. A. Stohlman, R. D. Atkinson, D. R. Hinton, and C. C. Bergmann. 2001. Acute CNS infection is insufficient to mediate chronic T cell retention. *Adv. Exp. Med. Biol.* **494**:349–354.
23. Marten, N. W., S. A. Stohlman, J. Zhou, and C. C. Bergmann. 2003. Kinetics of virus-specific CD8⁺-T-cell expansion and trafficking following central nervous system infection. *J. Virol.* **77**:2775–2778.
24. McMahon, E. J., S. L. Bailey, C. V. Castenada, H. Waldner, and S. D. Miller. 2005. Epitope spreading initiates in the CNS in two mouse models of multiple sclerosis. *Nat. Med.* **11**:335–339.
25. Mendez-Fernandez, Y. V., M. J. Hansen, M. Rodriguez, and L. R. Pease. 2005. Anatomical and cellular requirements for the activation and migration of virus-specific CD8⁺ T cells to the brain during Theiler's virus infection. *J. Virol.* **79**:3063–3070.
26. Murali-Krishna, K., J. D. Altman, M. Suresh, D. J. Sourdive, A. J. Zajac, J. D. Miller, J. Slansky, and R. Ahmed. 1998. Counting antigen-specific CD8 T cells: a reevaluation of bystander activation during viral infection. *Immunity* **8**:177–187.
27. Navas, S., and S. R. Weiss. 2003. Murine coronavirus-induced hepatitis: JHM genetic background eliminates A59 spike-determined hepatotropism. *J. Virol.* **77**:4972–4978.
28. Ontiveros, E., T. S. Kim, T. M. Gallagher, and S. Perlman. 2003. Enhanced virulence mediated by the murine coronavirus, mouse hepatitis virus strain JHM, is associated with a glycine at residue 310 of the spike glycoprotein. *J. Virol.* **77**:10260–10269.
29. Parra, B., D. R. Hinton, N. W. Marten, C. C. Bergmann, M. T. Lin, C. S. Yang, and S. A. Stohlman. 1999. IFN- γ is required for viral clearance from central nervous system oligodendroglia. *J. Immunol.* **162**:1641–1647.
30. Pewe, L., S. B. Heard, C. Bergmann, M. O. Dailey, and S. Perlman. 1999. Selection of CTL escape mutants in mice infected with a neurotropic coronavirus: quantitative estimate of TCR diversity in the infected central nervous system. *J. Immunol.* **163**:6106–6113.
31. Pewe, L., S. Xue, and S. Perlman. 1997. Cytotoxic T-cell-resistant variants arise at early times after infection in C57BL/6 but not in SCID mice infected with a neurotropic coronavirus. *J. Virol.* **71**:7640–7647.
32. Phillips, J. J., M. M. Chua, E. Lavi, and S. R. Weiss. 1999. Pathogenesis of chimeric MHV4/MHV-A59 recombinant viruses: the murine coronavirus spike protein is a major determinant of neurovirulence. *J. Virol.* **73**:7752–7760.
33. Phillips, J. J., M. M. Chua, G. F. Rall, and S. R. Weiss. 2002. Murine coronavirus spike glycoprotein mediates degree of viral spread, inflammation, and virus-induced immunopathology in the central nervous system. *Virology* **301**:109–120.
34. Rempel, J. D., S. J. Murray, J. Meisner, and M. J. Buchmeier. 2004. Differential regulation of innate and adaptive immune responses in viral encephalitis. *Virology* **318**:381–392.
35. Rempel, J. D., S. J. Murray, J. Meisner, and M. J. Buchmeier. 2004. Mouse hepatitis virus neurovirulence: evidence of a linkage between S glycoprotein expression and immunopathology. *Virology* **318**:45–54.
36. San Mateo, L. R., M. M. Chua, S. R. Weiss, and H. Shen. 2002. Perforin-mediated CTL cytotoxicity counteracts direct cell-cell spread of *Listeria monocytogenes*. *J. Immunol.* **169**:5202–5208.
37. Sarma, J. D., E. Scheen, S. H. Seo, M. Koval, and S. R. Weiss. 2002. Enhanced green fluorescent protein expression may be used to monitor murine coronavirus spread in vitro and in the mouse central nervous system. *J. Neurovirol.* **8**:381–391.
38. Scott, E. P., P. J. Branigan, A. M. Del Vecchio, and S. R. Weiss. 2008. Chemokine expression during mouse hepatitis virus-induced encephalitis: contributions of the spike and background genes. *J. Neurovirol.* **14**:5–16.
39. Shen, H., J. F. Miller, X. Fan, D. Kolwyck, R. Ahmed, and J. T. Harty. 1998. Compartmentalization of bacterial antigens: differential effects on priming of CD8 T cells and protective immunity. *Cell* **92**:535–545.
40. Stohlman, S. A., C. C. Bergmann, R. C. van der Veen, and D. R. Hinton. 1995. Mouse hepatitis virus-specific cytotoxic T lymphocytes protect from lethal infection without eliminating virus from the central nervous system. *J. Virol.* **69**:684–694.
41. Sutherland, R. M., M. M. Chua, E. Lavi, S. R. Weiss, and Y. Paterson. 1997. CD4⁺ and CD8⁺ T cells are not major effectors of mouse hepatitis virus A59-induced demyelinating disease. *J. Neurovirol.* **3**:225–228.
42. Trifilo, M. J., and T. E. Lane. 2004. The CC chemokine ligand 3 regulates CD11C⁺ CD11B⁺ CD8 α ⁻ dendritic cell maturation and activation following viral infection of the central nervous system: implications for a role in T cell activation. *Virology* **327**:8–15.
43. Wijburg, O. L., M. H. Heemskerk, A. Sanders, C. J. Boog, and N. Van Rooijen. 1996. Role of virus-specific CD4⁺ cytotoxic T cells in recovery from mouse hepatitis virus infection. *Immunology* **87**:34–41.